Selective Crystallization of d-Mannitol Polymorphs Using Surfactant Self-Assembly

Marques Penha, F.; Gopalan, A.; Meijlink, J.C.; Ibis, F.; Eral, H.B.

DOI
10.1021/acs.cgd.1c00243

Publication date
2021

Document Version
Final published version

Published in
Crystal Growth & Design

CRYSTAL GROWTH & DESIGN

pubs.acs.org/crystal

Article

Selective Crystallization of D-Mannitol Polymorphs Using Surfactant Self-Assembly

Frederico Marques Penha,[§] Ashwin Gopalan,[§] Jochem Christoffel Meijlink, Fatma Ibis, and Huseyin Burak Eral*

Cite This: *Cryst. Growth Des.* 2021, 21, 3928−3935

Read Online

ACCESS | Metrics & More | Article Recommendations | Supporting Information

ABSTRACT: Selective crystallization of polymorphs is highly sought after in industrial practice. Yet, state-of-the-art techniques either use laboriously engineered solid surfaces or strenuously prepared heteronucleants. We propose an approach where surfactants in solution self-assemble effortlessly into mesoscopic structures dictating the polymorphic outcome of the target solute. Sodium dodecyl sulfate (SDS) surfactant is used as a tailored additive to crystallize different polymorphic forms of a model active pharmaceutical ingredient, D-mannitol. Different mesoscopic phases of SDS template particular polymorphs: packed monolayers, micelles, and crystals favored the β, α, and δ forms of D-mannitol, respectively. A synergistic effect of topological templating and molecular interactions is proposed as the rationale behind the observed selective crystallization of polymorphs. This crystal engineering technique suggests that surfactant self-assemblies can be used as tailored templates for polymorphic control.

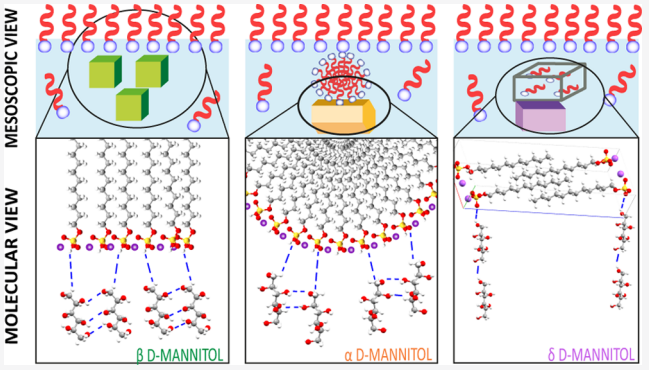

INTRODUCTION

Crystallization is a ubiquitous unit operation finding widespread application in the manufacturing of common table salt to functional nanostructured catalysts to essential medicines.[1] Despite being one of the predominantly downstream purification steps, the elementary phenomena of crystallization are far from being completely understood.[2−4] Particularly, primary nucleation has been extensively studied, yet its control still remains elusive. Primary nucleation plays a decisive role in determining product characteristics, such as crystal size distribution, shape, and polymorphic outcome of the new crystalline phase, in which crystal polymorphism may thwart the performance of the produced crystals.[5,6]

Polymorphism is the ability of a molecule to arrange itself in different crystal lattices, dictated by external conditions.[7] Selectively crystallizing a desired stable polymorph can be a major challenge in the pharmaceutical industry. The bioavailability of an active pharmaceutical ingredient (API) in the human body is intimately connected to the polymorphic form the API exhibits.[8] The late detection of a new polymorph after the commercial release of the antiviral drug, Ritonavir, remains a notorious example,[9] demonstrating what perils may arise from our inability to dictate and identify polymorphic forms.

Polymorph control has been extensively studied. Strategies based on controlling chemical interactions through a rational choice of solvents,[10,11] cosolvents,[12] physical parameters such as concentration,[13] evaporation rates,[14,15] as well as process conditions (cooling[16,17] and stirring rates[18]) are abundant in the literature. Weissbuch et al.[19] discuss the selective polymorph crystallization under the presence of tailor-made additives or impurities. In this context, an additive is an impurity deliberately added to the solution to somehow influence the nucleation of the growth process, being a common practice in several industries.[20] This is based on the hypothesis that, prior to nucleation, the molecules in supersaturated solutions form clusters in various shapes and arrangements, in which some might resemble the macroscopic crystal structure to be formed. The additive's structural and functional properties tailor to favor the crystal growth of the selected polymorph and inhibit other forms. This strategy was reported for several enantiomers and polymorphic forming crystals. The additive is selected for having stereochemistry similar enough to that of the unwanted polymorph/enantiomer. Due to this similarity, it will then adsorb onto the polymorph's fastest-growing face and prevent further growth, consequently favoring the growth of the desired form. The phenomenon was named as "rule of reversal".[21−23]

Received: March 2, 2021
Revised: May 11, 2021
Published: May 28, 2021

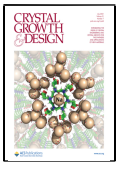

Over the last decades, using templated heterogeneous nucleation has gained traction in forming shelf-stable and bio-available polymorphs.[24] Heterogeneous nucleation, in general, is driven by the characteristics of the templates, including topography, surface functionality, and lattice matching between the crystal and substrate's lattices, favoring directional growth of the crystal.[1,19] The main advantage is that the templates can be tailored to produce the desired polymorphs. Solid heteronucleants, such as self-assembled monolayers (SAMs), on surfaces were reported to enhance nucleation, control polymorphs, and probe nucleation mechanisms.[25−33] Soft templates have also been reported by Diao et al.[34] that show the use of polymeric microgels with tunable pores to selectively crystallize polymorphs of carbamazepine and 5-methyl-2-[(2-nitrophenyl)amino]-3-thiophenecarbonitrile (ROY). The outcome was reported to be strongly influenced by the pore sizes and the chemical composition. Monolayer surfaces of amphiphilic molecules at the air−water interface were also reported to have an effect on inducing selective crystals of a given polymorph. The mechanism behind it was explained through partial structural similarity or electrostatic binding between the amphiphilic molecule's head group and the nucleating material.[19,35] Allen et al.[36] showed that the use of microemulsions and lamellar phases as soft templates under the presence of surfactants successfully induces different glycine polymorphs. The mechanism of the phenomenon was reported to be related to the binding of molecules at the oil−water interface rather than a templating effect on individual molecules. Following the same trend, Chen et al.[37] reported that different concentrations of sodium dodecyl sulfate (SDS) yield aragonite, vaterite, and calcite (calcium carbonate polymorphs), besides varying morphologies, yet no definitive mechanism was proposed.

Surfactants are commonly used in pharmaceutical formulation for increasing API solubilities[38,39] and in controlled drug delivery strategies.[40−42] Yet, the influence of surfactant self-assembled phases on primary nucleation remains underexplored. Surfactants are amphiphilic molecules which lower the interfacial tension between two repulsive fluid phases by aligning themselves favorably at the interface: hydrophilic head group interacts with the polar phase, while the hydrophobic tail group positions itself toward the nonpolar phase.[43] Using surfactants in the context of crystallization from solutions is promising as a single surfactant compound can self-assemble into structures at a mesoscale, that is, packed monolayer—at the air−solution interface—or micelles, and solid crystals can act as templates. Furthermore, if the template can be readily dissolved in the crystallizing solution, potential impurities originating from the addition of solid heteronucleants or seed crystals can be eliminated.

The model API used in this study, D-mannitol, has three known polymorphs (α, β, and δ) shown in Figure 1. The three polymorphs have varying stability at room temperature (RT) where the β form is the most stable and the δ form is the least. SDS is an anionic surfactant commonly used as an excipient in food and pharmaceutical manufacturing, provided it is used under its lethal dose (LD_{50}), and its use is approved by U.S. Food and Drug Administration (FDA).[44−46] Its head group comprises a sulfate ion and sodium as the counter-ion. The bulky tail is a 12-carbon long paraffin chain (Figure 1). Since SDS presents a Krafft point of 16 °C (where the critical micelle concentration of the surfactant is found equal to its solubility), higher when compared to other surfactants, it will exist as a

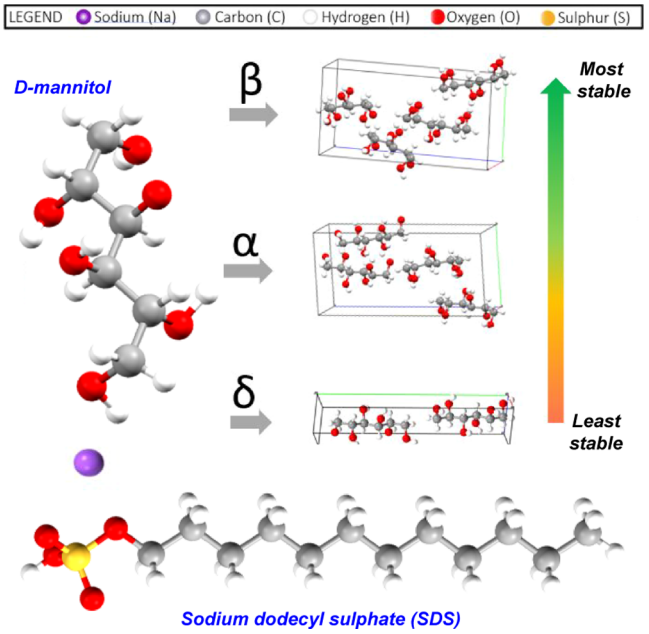

Figure 1. Chemical structure of D-mannitol along with its three polymorphs, α, β, and γ and the chemical structure of SDS.

hydrated crystal for the majority of the concentrations below this temperature. Above 16 °C, SDS will form micelles if above the critical micellar concentration (CMC—8.5 mM as shown in the Supporting Information and in accordance with the literature[47,48]) and form a monolayer at the air−solution interface in concentrations lower than the CMC. It is noteworthy that, despite being stable, micelles are a dynamic structure. This means that the monomers forming the micelles are continuously exchanged with the surrounding solution with a residence time in the order of microseconds in the micelle.[49] Despite that, surfactants have been reported to self-assemble as micelles even under shear stresses as high as 12,000 s^{-1}.[50] The shape of the micelles is the only parameter that has been reported to be influenced by hydrodynamic conditions, such as shear and flow rates.[51,52]

In this work, we explore the ability of SDS to selectively crystallize polymorphs of D-mannitol. To this end, we conduct cooling crystallization experiments at constant D-mannitol supersaturation (S = 2.5) at temperatures around SDS's Krafft point in three conditions: absence of SDS, a concentration well below the CMC, and a concentration well above the CMC. We hypothesized that intermolecular interactions between SDS and D-mannitol along with the templating effect of SDS mesoscale structures (monolayers and micelles) collectively dictate the polymorph crystallizing from solution. The presence of both H-bond donor (hydroxyl group hydrogen) and acceptor (hydroxyl group oxygen) atoms in D-mannitol and the presence of acceptor groups (sulfate group oxygen) on SDS makes H-bonding likely between these two molecules.[53] Furthermore, experiments conducted at different SDS concentrations at the same temperature enabled us to isolate the templating effect of self-assembled mesoscale structures of SDS such as micelles and surfactant monolayers. Such interfaces may induce preferential alignment of D-mannitol at interfaces, thus affecting polymorph selectivity. To test the proposed mechanism, we perform cooling crystallization experiments at different D-mannitol supersaturations in

https://doi.org/10.1021/acs.cgd.1c00243
Cryst. Growth Des. 2021, 21, 3928−3935

temperatures and concentrations around the SDS Krafft point to rationally switch between mesoscale SDS structures.

EXPERIMENTAL SECTION

Cooling Crystallization of D-Mannitol. Bulk solutions were prepared by adding distilled water to a required amount of D-mannitol (Merck—CAS: 69-65-8) and SDS (Sigma-Aldrich—CAS: 151-21-3). The solution was heated in a hot plate at 70 °C for 30 min under stirring to ensure complete dissolution. 3 mL aliquots of the homogeneous solution were then transferred to glass screw vials, compatible with Crystalline (Technobis Crystallization Systems). Each cooling crystallization cycle consisted of four steps: a temperature ramp from the crystallization temperature (T_c) to 70 °C with a fast heating rate of 5 °C/min; a hold period of 30 min at 70 °C; a temperature ramp from 70 °C to T_c at a cooling rate of 5 °C/min; and, finally, a hold period of 120 min at T_c as shown in Figure 2.

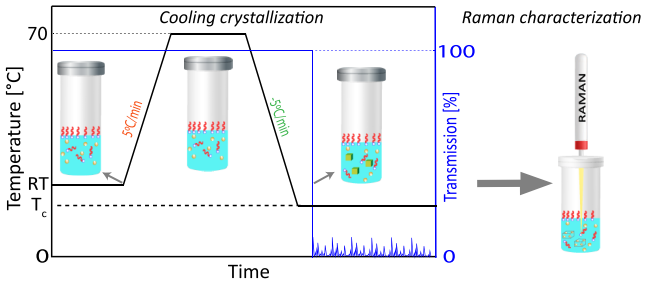

Figure 2. Illustration of the experimental procedure for cooling crystallization experiments and characterization. An aqueous stock solution containing D-mannitol and SDS is first dissolved at 70 °C (not shown). Aliquots of homogeneous solutions are crystallized according to the temperature profile provided, starting at room temperature (RT) and ending at the proposed crystallization temperature (T_c). The resulting suspended crystals are characterized by Raman spectroscopy.

The stirring speed was maintained at 700 rpm to ensure uniform mixing. The heating and cooling rates were fixed for all experiments. A longer hold time of 2 h after the cooling step was used to ensure sufficient time for nucleation. The experiments are summarized in Table 1. Three sets of crystallization experiments were performed,

Table 1. Experimental Conditions

temperature [°C]	experiments	D-mannitol	SDS [g]	SDS form [g]
25	no SDS	13.1		
	0.1 wt % SDS		0.025	monomers
	1.22 wt % SDS		0.306	micelles
15	no SDS	10		
	0.1 wt % SDS		0.025	monomers
	1.22 wt % SDS		0.306	micelles
5	no SDS	8.5		
	0.1 wt % SDS		0.025	monomers
	1.22 wt % SDS		0.306	crystals

each at a crystallization temperature (T_c): 25, 15, and 5 °C. In these experiments, depending on the concentration, SDS exists as micelles at 25 and 15 °C, as crystals at 5 °C, and as monomers at all temperatures (Table 1). We have chosen to keep supersaturation of D-mannitol (S = 2.5) constant. This decision is based on the reasonably fast nucleation kinetics obtained for D-mannitol at this supersaturation. The amount of D-mannitol to be added is calculated based on the solubility data provided in the Supporting Information (Table 1).

The crystallized vials were immediately characterized with the Raman spectroscopy (Kaiser Raman Rxn2 analyzer). The probe was directly introduced in the vials and was kept approximately 3 mm away from the surface of the sedimented crystals. Main parameters including exposure time (10 s) and sample collection time (120 s) were adjusted to achieve accurate measurements for each sample. The intensity peaks are plotted against the Raman shift [cm^{-1}]. Each crystal possesses different electron densities in various vibrational modes; thus, the intensity peaks obtained at unique Raman shifts can be used to identify the polymorph. At least 24 vials were crystallized for each set of experiments. Raman measurements were obtained for each vial and compared to standards to identify the polymorphic outcome.

Preparation of SDS Seeds. Two types of SDS seeds have been used for the seeded cooling crystallization experiments: the stock SDS and SDS crystals produced by recrystallizing SDS in aqueous solutions. Recrystallized SDS was produced in bulk using an automated reactor (EasyMax 402, Mettler Toledo). An aqueous solution with 30 wt % SDS was prepared and subjected to a cooling crystallization profile: a temperature ramp to 50 °C at a heating rate of 5 °C/min to dissolve the SDS; a hold step at 50 °C for a period of 30 min; a ramp to 5 °C at a cooling rate of 5 °C/min; and a final hold step at 5 °C for a period of 60 min. The stirring was set at 150 rpm. The resulting recrystallized product was filtered, and the removed crystals were kept in the oven at 40 °C for 24 h. These crystals were finely ground with pestle and mortar before being utilized in the seeding experiments. X-ray powder diffraction (D2 phaser, Bruker) was used to characterize the SDS seeds in both the stock and recrystallized seeds.

Seeded Cooling Crystallization of D-Mannitol. The seeding crystallization experiments were performed using the same materials and procedure as the cooling crystallization experiments, except for the addition of seeds. Seeds were introduced at 10 °C, and the seeding load was maintained at 1.22 wt % SDS. This seeding point was chosen because, at this temperature, D-mannitol would still be in the metastable zone, and the SDS seeds would only dissolve slightly at this temperature (1.22 wt % SDS crystals were found to dissolve completely only at around 12.3 °C—details are provided in the Supporting Information). Different supersaturated solutions of D-mannitol (S = 2.3, 2.5, and 2.95) were prepared in bulk and subjected to the same cooling cycle, only with a final hold period of 60 min at 5 °C.

RESULTS AND DISCUSSION

Figure 3 summarizes the experiments carried out at constant D-mannitol supersaturation, $S = c/c_{sat}$ = 2.5, at 25, 15, and 5 °C at three SDS concentrations: in the absence of SDS, a concentration well below the CMC (0.1 wt %), and a concentration well above the CMC (1.22 wt %). Considering the experiments devoid of SDS (Figure 3A), the majority of the experiments either returned pure β and δ forms or a mixture of β and δ forms (from this point on, referred simply as "mixture"). When a small amount of SDS (0.1 wt %) was added, a significant increase in the β form with decreased mixture percentage was noted at all temperatures (Figure 3B). In the next set of experiments given in Figure 3C with 1.22 wt % SDS, samples crystallized produced a majority of β polymorphs at 25 and 15 °C. Surprisingly, an onset of the α form was also observed at 25 and 15 °C, while a large increase in the proportion of the δ polymorph was seen at 5 °C.

The first inference that could be drawn is that in the absence of SDS, D-mannitol does not have a preferred polymorph (Figure 3a). In the presence of SDS both above CMC and below CMC, it appears that the addition of SDS does not steer the solutions toward a given polymorph completely at all three temperatures (Figure 3B,C). However, on further analysis, a pattern can be deciphered in terms of the polymorph

https://doi.org/10.1021/acs.cgd.1c00243
Cryst. Growth Des. 2021, 21, 3928−3935

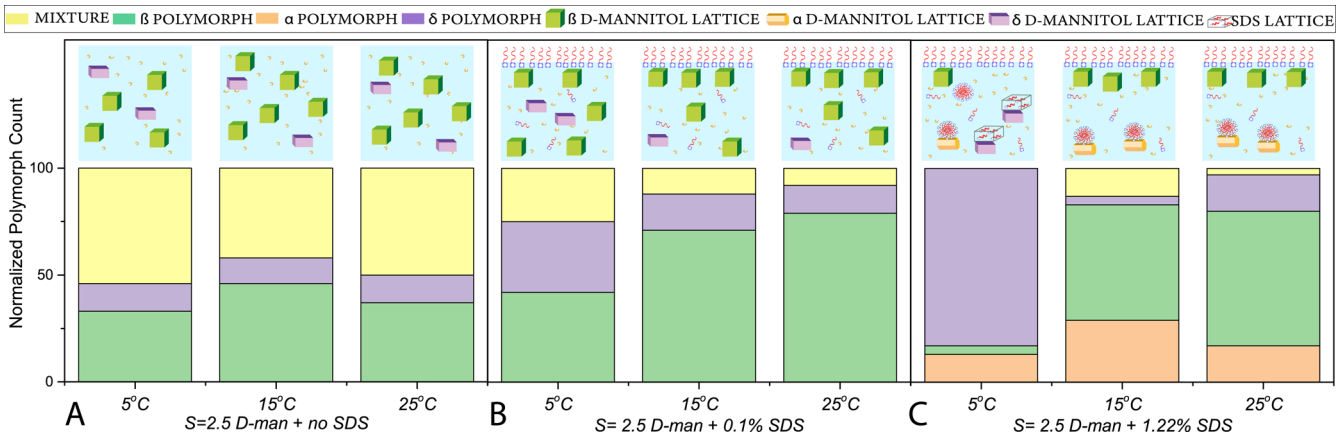

Figure 3. Distribution of polymorphs crystallizing in cooling crystallization experiments at different temperatures and SDS concentrations at fixed D-mannitol supersaturation (S = 2.5). Note that the term "mixture" indicates some proportion of β and δ in the vial.

distribution. D-Mannitol exhibits an enantiotropic relationship between δ and β-D-mannitol.[54] Thus, considering Ostwald's rule of stages,[1,8] it is possible that the unstable δ form nucleates first and subsequently transforms to the stable β form. This would provide an explanation as to why abundant mixture (of β and δ) and pure β form were obtained in the absence of SDS. Another explanation for observing a mixture of different polymorphs could be because of the concomitant crystallization of these two D-mannitol polymorphs. Concomitant crystallization of different polymorphs is not an uncommon phenomenon. Simultaneous crystallization has been observed in other polymorphic systems, for example, cooling crystallization of L-glutamic acid yielded both α and β forms under certain mixing and supersaturation conditions.[55] D-Mannitol has also been found to exhibit concomitant polymorphism when melt crystallization was performed.[56] The α polymorph, in its turn, presents a monotropic relation with the other two, thus reversal stability until their melting point is not expected.[54,57]

Based on the observations summarized in Figure 3, we hypothesize that the presence of SDS as monomers (or a monolayer at the air−solution interface) would favor the formation of the β form. SDS as a micelle present at 25 and 15 °C at 1.22 wt % favored the crystallization of the α form and consequently reduced the β form at both temperatures. Moreover, since higher proportions of the δ polymorph are favored at high SDS concentration and lower temperature (1.22 wt % and 5 °C), under which conditions SDS crystallizes, the presence of SDS as crystals would favor the formation of the δ polymorph.

In order to explore whether an increase in SDS micelle concentration would increase the proportion of the α form, new experiments were performed using 2.44 and 5 wt % of SDS provided in Figure 4. At these SDS concentrations, more SDS micelles would be present in the solution. This hypothesis was tested with the same D-mannitol supersaturation S = 2.5 at 25 and 15 °C. The results in Figure 4 show that, indeed, the increase in the concentration of SDS in temperature conditions where it exists as a micelle favors the formation of α D-mannitol. The higher concentration of SDS (5 wt %) yielded over 87% of the vials crystallized at 15 °C as α-mannitol. Yet, a smaller proportion of the vials still crystallizes as the stable β form.

To further investigate whether SDS crystals could favor the formation of a δ polymorph, cooling crystallization experiments were conducted at 5 °C with solutions containing identical SDS concentration, that is, 1.22 wt % of SDS, yet different D-mannitol supersaturations. The induction time (τ) taken by the crystals to nucleate and grow to detectable sizes[58] of D-mannitol at each supersaturation and of 1.22 wt % SDS in their pure solutions were measured. Under these conditions (1.22 wt % and 5 °C), the solutions containing SDS micelles will undergo crystallization. Hence, through the comparison of the induction time of SDS with different supersaturated solutions of D-mannitol, it can be speculated which heteronucleant phase would be responsible for the obtained polymorph distribution. With reference to the original S = 2.5 solution at 5 °C, two other supersaturated solutions were chosen: a higher supersaturation at S = 2.95 (400 g/L) and a lower supersaturation at S = 2.3 (312 g/L). These pure D-mannitol and SDS solutions were subjected to the same cooling crystallization cycle shown in Figure 2 using Crystalline. Over 24 vials were crystallized for each of the new supersaturations tested. The results are shown in Table 2.

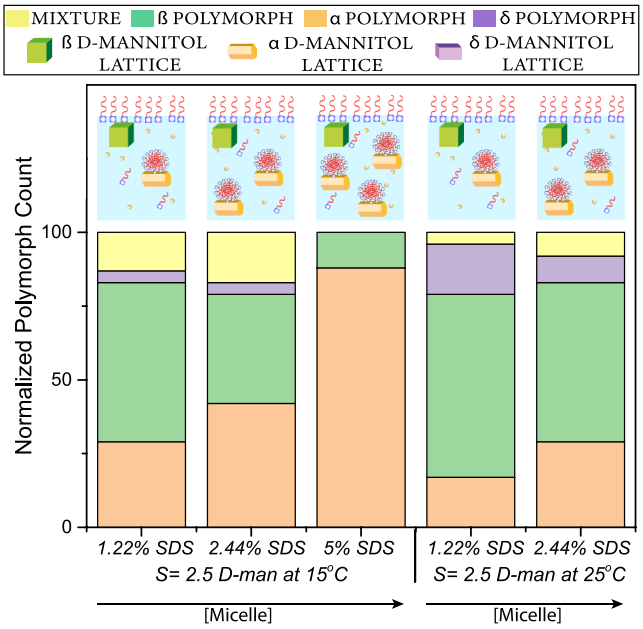

Figure 4. Distribution of polymorphs crystallizing in cooling crystallization experiments varying the SDS concentrations at fixed D-mannitol supersaturation, S = 2.5 with 15 and 25 °C.

https://doi.org/10.1021/acs.cgd.1c00243
Cryst. Growth Des. 2021, 21, 3928−3935

Table 2. Induction Times of Pure SDS and D-Mannitol Solutions in Different Supersaturations at 5 °C

	D-mannitol			SDS
supersaturation	S = 2.95	S = 2.5	S = 2.3	1.22 wt %
induction time [s]	116 ± 0.6	408 ± 2.5	867 ± 8.5	472 ± 0.5

Comparing the pure D-mannitol and SDS induction times, it can be stated that D-mannitol solutions with S = 2.95 and 2.3 nucleate, respectively, much faster and much slower than the solution containing only SDS. Original D-mannitol solution with S = 2.5 showed comparable induction times with the SDS pure solution. Detailed information on obtaining of the induction time is given in the Supporting Information.

Results shown in Figure 5 can be correlated with the observed induction times. The first set of experiments at S = 2.95, D-mannitol with 1.22 wt % SDS yielded predominantly the α form. Since at S = 2.95, D-mannitol nucleates much faster than SDS, this would indicate that micelles form when D-mannitol nucleates. As SDS micelles were seen to favor the α form, a high percentage of α forms is observed. S = 2.5 yields a very high percentage of δ forms probably due to comparable induction times for SDS and mannitol. At this concentration, SDS and D-mannitol were seen to nucleate almost simultaneously. Thus, both SDS crystals and micelles could successively act as heteronucleants favoring a high percentage of δ. Yet, a percentage of α forms was still observed. The last set of experiments, at S = 2.3 D-mannitol, strengthens the proposed correlation regarding the role of the SDS crystal template. As SDS nucleates earlier D-mannitol, the formed SDS crystals might act as a heteronucleant template for selective polymorphism of the δ form. It is noteworthy that the crystals were analyzed using Raman spectroscopy immediately after their formation. Due to the enantiotropic relation between δ and β polymorphs and considering the higher stability of β at this temperature, a polymorph transition might also be possible. Nonetheless, only δ-D-mannitol nucleated.

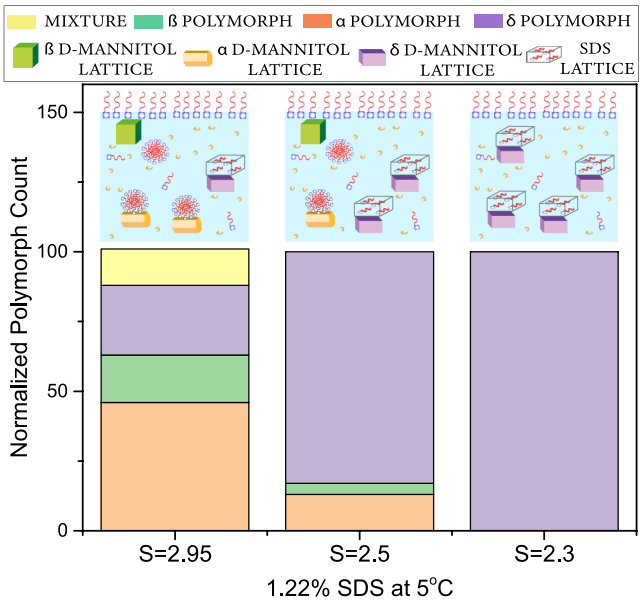

Figure 5. Distribution of polymorphs crystallizing from solutions with different D-mannitol supersaturation at 5 °C, while the SDS concentration is fixed at 1.22 wt %.

To further examine the hypothesis that SDS crystals predominantly favored the δ polymorph, seeded experiments were performed at 5 °C, in the same supersaturations (S = 2.3, 2.5, and 2.95) using stock and freshly prepared SDS seeds. Both seeds comprise a mixture of different SDS hydrates (more information is given in the Supporting Information). As can be seen in Figure 6, whether used as-is from the manufacturer or freshly prepared by recrystallization, the presence of seeds greatly increased the formation of δ D-mannitol in all supersaturations tested. This shows a marked improvement compared to the previous results in Figure 4, where S = 2.95 did not produce a high percentage of δ forms. We attribute the ability of both stock and recrystallized SDS seeds to selectively crystallize δ-D-mannitol to their ability to form H-bonds through the sulfate group.

In order to consolidate these claims, seeding experiments were repeated with another surfactant seed [cetyltrimethylammonium bromide (CTAB)]. CTAB was chosen due to its many similarities to SDS: it also exists as a crystal at 5 °C[59] and, being a cationic surfactant with the presence of ammonium bromide in the head group, it also establishes dipole−dipole interaction with D-mannitol. Thus, CTAB represents a surface template exhibiting similar properties to SDS. The results obtained for seeding crystallization experiments with 1.22 wt % CTAB seeds are also shown in Figure

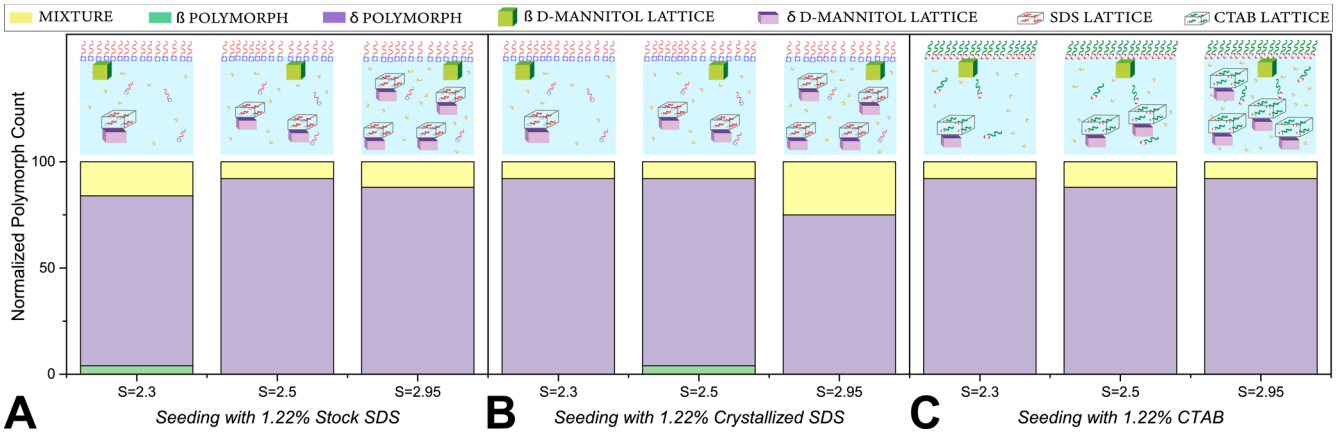

Figure 6. Distribution of polymorphs crystallizing from seeded cooling crystallization experiments at various supersaturations with seeds from the manufacturer, recrystallized SDS seeds, and CTAB seeds.

https://doi.org/10.1021/acs.cgd.1c00243
Cryst. Growth Des. 2021, 21, 3928−3935

6C. Like the SDS seeds, the CTAB seeds also predominantly favor the δ polymorph. However, in both cases, a 100% δ form could not be obtained. One reason for that might be the polydisperse nature of the added CTAB/SDS seeds. The randomized topology of these seeds might result in inconsistent availability of surface area required for δ-D-mannitol and hence could result in a polymorph mixture. Another possibility for the presence of mixtures would be the transition from δ to β form.

The results presented in Figures 3−6 indicate that in the presence of SDS monomers, micelles, and crystals, β-, α-, and δ-D-mannitol are, respectively, favored. Since heterogeneous nucleation can be aided by multiple mechanisms, namely, intermolecular interactions and topological/confinement effects of the substrate (SDS) on the overlayer (D-mannitol), a mechanistic role of SDS is proposed. Crystal nucleation is reported to proceed by the initial formation of conformers followed by ordered rearrangement into lattices.[60−62] Thus, studying the conformer alignment at a molecular level could help in understanding how the D-mannitol molecule relates to the interface and subsequently forms a polymorph.

The SDS molecule could exist in solution as a monomer, a packed monolayer at the air−solution interface, or a micelle depending on the concentration and temperature.[63] In self-assembled mesoscopic structures, such as monolayers and micelles, the D-mannitol molecule has to interact with the SDS head group sticking out toward the aqueous solution. Dissolved SDS molecules exhibit pronounced intermolecular interactions due to their ability to form ion-dipole and H-bond interactions using the sulfate ion.[53] As D-mannitol also comprises H-bonding sites in the form of six hydroxyl groups (−OH), intermolecular interaction between these molecules favoring directional growth of D-mannitol crystal is a possibility. Previous studies have also reported the role of hydrogen bonding between the target compound and the substrate SAM in facilitating nucleation, promoting oriented crystal growth, and controlling polymorphic outcome.[19,25,26,35] Su and coworkers[64] report the nucleation of D-mannitol polymorphs through molecular dynamic simulations on aqueous solutions in different concentrations, from undersaturated to supersaturated solutions. It was reported that, from supersaturated aqueous solutions of D-mannitol, the terminal hydroxyl groups of D-mannitol have a higher propensity to establish H-bonds with water. The same study also points out the formation of different D-mannitol dimers in solution which eventually turn into crystals of different polymorphs of D-mannitol, in which β-D-mannitol has been particularly found to be favored by a body−body dimer, α-D-mannitol was reported to be favored by the body−tail dimer, and a tail−tail dimer was related to the δ-D-mannitol.

In this sense, there is a possibility that a parallel arrangement of D-mannitol molecules is induced by the particular H-bonds formed with the SDS monolayer. Along the same lines, the increase in the α-D-mannitol observed with increasing concentrations of SDS at 25 and 15 °C might be caused by the H-bonds formed at the curve surface of the micelle, which could possibly favor a different dimer formation. As both α- and β-D-mannitol exhibit an orthorhombic lattice, minor changes in their hydroxyl group orientation and a consequent change in the formed dimer could prompt crystallization of different polymorphs. SDS crystals, which we call "hard" heteronucleants, induced preferentially the most unstable of D-mannitol's polymorphs (δ) under a crystallization temperature of 5 °C as shown in Figure 6. Different features of the surface could play a role in favoring nucleation. Since there is a large size difference between surfactants and D-mannitol's unit cell, a confinement effect could be the reason for aligning D-mannitol molecules on top of its hard crystalline surface. Furthermore, D-mannitol molecule might interpret the surfactants' unit cells (both SDS and CTAB) as flat interfaces, whether they are introduced as seeds or formed in situ during cooling crystallization in situ. Due to the significant size difference between the surfactant and D-mannitol lattices (ratio of SDS·1/8H_2O and δ D-mannitol lattice are of the order 1:10), D-mannitol molecules could interpret the seed as SDS/CTAB molecules placed at a distance. Thus, the dearth of adjacent dipole sites might facilitate a terminal alignment of D-mannitol molecules which subsequently favors δ-D-mannitol. Nonetheless, this discussion provides a possible direction toward unveiling the mechanism that needs further confirmation with both experimental and molecular dynamics simulation approaches.

CONCLUSIONS

In this study, we use distinct SDS self-assemblies (monolayer, micelle, and crystal) as designed heteronucleant templates to selectively crystallize D-mannitol in cooling crystallization. Our experimental evidence points out that distinct SDS self-assemblies can trigger the crystallization of different D-mannitol polymorphs. We dictate which SDS heteronucleant self-assembles in a homogeneous solution containing SDS and D-mannitol by controlling the crystallization temperature and SDS concentration. The stable β polymorph of D-mannitol was favored in the presence of the SDS monolayer forming at the air−solution interface, while the presence of SDS micelles promoted the preferential crystallization of the metastable α-D-mannitol. We speculate that self-assembled mesoscopic "soft" structures such as monolayers and micelles facilitate the alignment of the solute interacting with a flat SDS monolayer or with a curved micelle interface, thus inducing, respectively, α and β-D-mannitol. Finally, the presence of hard SDS crystal templates was seen to selectively induce a higher proportion of the unstable δ-D-mannitol likely due to combined effects of surface confinement and intermolecular interactions.

In the formation of all three polymorphs, the synergistic effect of self-assembled structure's surface topology and intermolecular bonding is hypothesized to play a crucial role in determining the resulting polymorph. This study provides experimental evidence that polymorphism of a solute molecule can be controlled by tailoring the self-assembly of a surfactant to act as a heteronucleant. In doing so, it provides a step forward onto a previously underexplored approach to tailor the stability and bio-availability of APIs and adds a valuable tool to extend our understanding of polymorphism.

ASSOCIATED CONTENT

Supporting Information

The Supporting Information is available free of charge at https://pubs.acs.org/doi/10.1021/acs.cgd.1c00243.

Detailed information on Solubility of D-mannitol, Raman characterization, microscopic characterization, solubility estimation of SDS, effect of D-mannitol on the CMC of SDS, effect of D-mannitol on the solubility of SDS, induction time measurements and SDS hydrates profile (PDF)

https://doi.org/10.1021/acs.cgd.1c00243
Cryst. Growth Des. 2021, 21, 3928−3935

AUTHOR INFORMATION

Corresponding Author

Huseyin Burak Eral − *Process & Energy Department, Delft University of Technology, 2628 CB Delft, The Netherlands;* orcid.org/0000-0003-3193-452X; Email: h.b.eral@tudelft.nl

Authors

Frederico Marques Penha − *Department of Chemical Engineering, KTH Royal Institute of Technology, SE100-44 Stockholm, Sweden; Process & Energy Department, Delft University of Technology, 2628 CB Delft, The Netherlands;* orcid.org/0000-0001-7614-8448

Ashwin Gopalan − *Process & Energy Department, Delft University of Technology, 2628 CB Delft, The Netherlands*

Jochem Christoffel Meijlink − *Process & Energy Department, Delft University of Technology, 2628 CB Delft, The Netherlands*

Fatma Ibis − *Process & Energy Department, Delft University of Technology, 2628 CB Delft, The Netherlands*

Complete contact information is available at: https://pubs.acs.org/10.1021/acs.cgd.1c00243

Author Contributions

[§]F.M.P. and A.G. contributed equally. The manuscript was written through the contributions of all authors. All authors have given approval to the final version of the manuscript.

Notes

The authors declare no competing financial interest.

ACKNOWLEDGMENTS

This project has received funding from the European Union's Horizon 2020 research and innovation programme under the Marie Skłodowska-Curie grant agreement no 707404. The opinions expressed in this document reflect only the author's views. The European Commission is not responsible for any use that may be made of the information it contains.

REFERENCES

(1) Thakore, S. D.; Sood, A.; Bansal, A. K. Emerging role of primary heterogeneous nucleation in pharmaceutical crystallization. *Drug Dev. Res.* **2020**, *81*, 3−22.

(2) Myerson, A. S.; Trout, B. L. Nucleation from solution. *Science* **2013**, *341*, 855−856.

(3) Meldrum, F. C.; Sear, R. P. Now you see them. *Science* **2008**, *322*, 1802−1803.

(4) Lévesque, A.; Maris, T.; Wuest, J. D. ROY Reclaims Its Crown: New Ways To Increase Polymorphic Diversity. *J. Am. Chem. Soc.* **2020**, *142*, 11873−11883.

(5) Garside, J.; Davey, R. J. *From Molecules to Crystallizers*; Oxford: U.K., 2001.

(6) Vekilov, P. G. Nucleation of protein crystals. *Prog. Cryst. Growth Charact. Mater.* **2016**, *62*, 136−154.

(7) Lewis, A.; Seckler, M.; Kramer, H.; van Rosmalen, G. *Industrial Crystallization*; Cambrige University Press: Cambridge, 2015; pp 323.

(8) Lee, E. H. A practical guide to pharmaceutical polymorph screening & selection. *Asian J. Pharm. Sci.* **2014**, *9*, 163−175.

(9) Chemburkar, S. R.; Bauer, J.; Deming, K.; Spiwek, H.; Patel, K.; Morris, J.; Henry, R.; Spanton, S.; Dziki, W.; Porter, W.; Quick, J.; Bauer, P.; Donaubauer, J.; Narayanan, B. A.; Soldani, M.; Riley, D.; McFarland, K. Dealing with the impact of ritonavir polymorphs on the last stages of bulk drug process development. *Org. Process Res. Dev.* **2000**, *4*, 413−417.

(10) Svärd, M.; Rasmuson, Å. C. M-hydroxybenzoic acid: Quantifying thermodynamic stability and influence of solvent on the nucleation of a polymorphic system. *Cryst. Growth Des.* **2013**, *13*, 1140−1152.

(11) Shi, P.; Xu, S.; Du, S.; Rohani, S.; Liu, S.; Tang, W.; Jia, L.; Wang, J.; Gong, J. Insight into solvent-dependent conformational polymorph selectivity: The case of undecanedioic acid. *Cryst. Growth Des.* **2018**, *18*, 5947−5956.

(12) Gong, N.; Wang, X.; Wang, Y.; Yang, S.; Song, J.; Lu, Y.; Du, G. Control over Polymorph Formation of Polydatin in Binary Solvent System and Structural Characterization. *J. Pharm. Biomed. Anal.* **2020**, *190*, 113260.

(13) Su, W.; Hao, H.; Glennon, B.; Barrett, M. Spontaneous polymorphic nucleation of d -mannitol in aqueous solution monitored with Raman spectroscopy and FBRM. *Cryst. Growth Des.* **2013**, *13*, 5179−5187.

(14) Lu, B.; Liu, S.; Yan, D. Recent advances in photofunctional polymorphs of molecular materials. *Chin. Chem. Lett.* **2019**, *30*, 1908−1922.

(15) Tian, F.; Qu, H.; Louhi-Kultanen, M.; Rantanen, J. Mechanistic insight into the evaporative crystallization of two polymorphs of nitrofurantoin monohydrate. *J. Cryst. Growth* **2009**, *311*, 2580−2589.

(16) Sudha, C.; Srinivasan, K. Nucleation control and separation of paracetamol polymorphs through swift cooling crystallization process. *J. Cryst. Growth* **2014**, *401*, 248−251.

(17) Rhoades, A. M.; Wonderling, N.; Gohn, A.; Williams, J.; Mileva, D.; Gahleitner, M.; Androsch, R. Effect of cooling rate on crystal polymorphism in beta-nucleated isotactic polypropylene as revealed by a combined WAXS/FSC analysis. *Polymer* **2016**, *90*, 67−75.

(18) Vesga, M. J.; McKechnie, D.; Mulheran, P. A.; Johnston, K.; Sefcik, J. Conundrum of γ glycine nucleation revisited: to stir or not to stir? *CrystEngComm* **2019**, *21*, 2234−2243.

(19) Weissbuch, I.; Lahav, M.; Leiserowitz, L. Understanding of Crystal Nucleation, Monitoring, and Understanding of Crystal Nucleation. *Cryst. Growth Des.* **2003**, *3*, 125−150.

(20) Sangwal, K. *Additives and Crystallization Processes in Industries*, 2007; pp 319−379.

(21) Addadi, L.; Weinstein, S.; Gati, E.; Weissbuch, I.; Lahav, M. Resolution of Conglomerates with the Assistance of Tailor-made Impurities. Generality and Mechanistic Aspects of the "Rule of Reversal". A New Method for Assignment of Absolute Configuration. *J. Am. Chem. Soc.* **1982**, *104*, 4610−4617.

(22) Addadi, L.; Berkovitch-Yellin, Z.; Domb, N.; Gati, E.; Lahav, M.; Leiserowitz, L. Resolution of conglomerates by stereoselective habit modifications. *Nature* **1982**, *296*, 21−26.

(23) Weissbuch, I.; Lahav, M. Crystalline architectures as templates of relevance to the origins of homochirality. *Chem. Rev.* **2011**, *111*, 3236−3267.

(24) Parambil, J. V.; Poornachary, S. K.; Heng, J. Y. Y.; Tan, R. B. H. Template-induced nucleation for controlling crystal polymorphism: From molecular mechanisms to applications in pharmaceutical processing. *CrystEngComm* **2019**, *21*, 4122−4135.

(25) Frostman, L. M.; Bader, M. M.; Ward, M. D. Nucleation and Growth of Molecular Crystals on Self-Assembled Monolayers. *Langmuir* **1994**, *10*, 576−582.

(26) Carter, P. W.; Ward, M. D. Directing Polymorph Selectivity During Nucleation of Anthranilic Acid on Molecular Substrates. *J. Am. Chem. Soc.* **1994**, *116*, 769−770.

(27) Boyes, M.; Alieva, A.; Tong, J.; Nagyte, V.; Melle-Franco, M.; Vetter, T.; Casiraghi, C. Exploiting the Surface Properties of Graphene for Polymorph Selectivity. *ACS Nano* **2020**, *14*, 10394−10401.

(28) Cui, Y.; Stojakovic, J.; Kijima, H.; Myerson, A. S. Mechanism of Contact-Induced Heterogeneous Nucleation. *Cryst. Growth Des.* **2016**, *16*, 6131−6138.

(29) Kang, J. F.; Zaccaro, J.; Ulman, A.; Myerson, A. Nucleation and growth of glycine crystals on self-assembled monolayers on gold. *Langmuir* **2000**, *16*, 3791−3796.

(30) Tulli, L. G.; Moridi, N.; Wang, W.; Helttunen, K.; Neuburger, M.; Vaknin, D.; Meier, W.; Shahgaldian, P. Polymorphism control of an active pharmaceutical ingredient beneath calixarene-based Langmuir monolayers. *Chem. Commun.* **2014**, *50*, 3938−3940.
(31) Yang, H.; Song, C. L.; Lim, Y. X. S.; Chen, W.; Heng, J. Y. Y. Selective crystallisation of carbamazepine polymorphs on surfaces with differing properties. *CrystEngComm* **2017**, *19*, 6573−6578.
(32) Price, C. P.; Grzesiak, A. L.; Matzger, A. J. Crystalline polymorph selection and discovery with polymer heteronuclei. *J. Am. Chem. Soc.* **2005**, *127*, 5512−5517.
(33) Briseno, A. L.; Aizenberg, J.; Han, Y.-J.; Penkala, R. A.; Moon, H.; Lovinger, A. J.; Kloc, C.; Bao, Z. Patterned growth of large oriented organic semiconductor single crystals on self-assembled monolayer templates. *J. Am. Chem. Soc.* **2005**, *127*, 12164−12165.
(34) Diao, Y.; Whaley, K. E.; Helgeson, M. E.; Woldeyes, M. A.; Doyle, P. S.; Myerson, A. S.; Hatton, T. A.; Trout, B. L. Gel-induced selective crystallization of polymorphs. *J. Am. Chem. Soc.* **2012**, *134*, 673−684.
(35) Kuzmenko, I.; Rapaport, H.; Kjaer, K.; Als-Nielsen, J.; Weissbuch, I.; Lahav, M.; Leiserowitz, L. Design and characterization of crystalline thin film architectures at the air-liquid interface: Simplicity to complexity. *Chem. Rev.* **2001**, *101*, 1659−1696.
(36) Allen, K.; Davey, R. J.; Ferrari, E.; Towler, C.; Tiddy, G. J.; Jones, M. O.; Pritchard, R. G. The Crystallization of Glycine Polymorphs from Emulsions, Microemulsions, and Lamellar Phases. *Cryst. Growth Des.* **2002**, *2*, 523−527.
(37) Chen, Z.; Li, C.; Yang, Q.; Nan, Z. Transformation of novel morphologies and polymorphs of CaCO3 crystals induced by the anionic surfactant SDS. *Mater. Chem. Phys.* **2010**, *123*, 534−539.
(38) Nachari, Y.; Jabbari, M. A case study on the partitioning of pharmaceutical compound naproxen in edible oil-water system in the presence of ionic and non-ionic surfactants. *J. Taiwan Inst. Chem. Eng.* **2021**, *119*, 1−5.
(39) Stoyanova, K.; Vinarov, Z.; Tcholakova, S. Improving Ibuprofen solubility by surfactant-facilitated self-assembly into mixed micelles. *J. Drug Deliv. Sci. Technol.* **2016**, *36*, 208−215.
(40) Chen, S.; Hanning, S.; Falconer, J.; Locke, M.; Wen, J. Recent advances in non-ionic surfactant vesicles (niosomes): Fabrication, characterization, pharmaceutical and cosmetic applications. *Eur. J. Pharm. Biopharm.* **2019**, *144*, 18−39.
(41) Fenton, T.; Kanyuck, K.; Mills, T.; Pelan, E. Formulation and characterisation of kappa-carrageenan gels with non-ionic surfactant for melting-triggered controlled release. *Carbohydr. Polym. Technol. Appl.* **2021**, *2*, 100060.
(42) Fetih, G. Fluconazole-loaded niosomal gels as a topical ocular drug delivery system for corneal fungal infections. *J. Drug Deliv. Sci. Technol.* **2016**, *35*, 8−15.
(43) Israelachvilli, J. N. *Intermolecular and Surface Forces*; Elsevier, 2011.
(44) Suhail, M.; Janakiraman, A. K.; Khan, A.; Naeem, A.; Badshah, S. F. Surfactants and their role in Pharmaceutical Product Development: An Overview. *J. Pharm. Pharm.* **2019**, *6*, 72−82.
(45) Bondi, C. A. M.; Marks, J. L.; Wroblewski, L. B.; Raatikainen, H. S.; Lenox, S. R.; Gebhardt, K. E. Human and environmental toxicity of sodium lauryl sulfate (SLS): Evidence for safe use in household cleaning products. *Environ. Health Insights* **2015**, *9*, No. ehi.s31765.
(46) Sheskey, P. J.; Cook, W. G.; Cable, C. G. *Handbook of Pharmaceutical Excipients*, 8th ed.; Pharmaceutical Press, 2017; p 1216.
(47) Chatterjee, A.; Moulik, S. P.; Sanyal, S. k.; Mishra, B. K.; Puri, P. M. Thermodynamics of micelle formation of ionic surfactants: A critical assessment for sodium dodecyl sulfate, cetyl pyridinium chloride and dioctyl sulfosuccinate by microcalorimetric, conductometric and tensiometric measurements. *J. Phys. Chem. B* **2001**, *105*, 12823−12831.
(48) Holmberg, K.; Shah, D. O.; Schwuger, M. J. *Handbook of Applied Surface and Colloid Chemistry*; John Wiley & Sons, 2002.
(49) Fuhrhop, J. H.; Koning, J. *Membranes and Molecular Assemblies: The Synkinetic Approach*; Royal Society of Chemistry, 2007. ISSN.
(50) Kalus, J.; Hoffmann, H.; Chen, S. H.; Lindner, P. Correlations in micellar solutions under shear: A small-angle neutron scattering study of the chain surfactant N-hexadecyloctyldimethylammonium bromide. *J. Phys. Chem.* **1989**, *93*, 4267−4276.
(51) Buckinx, A. L.; Verstraete, K.; Baeten, E.; Tabor, R. F.; Sokolova, A.; Zaquen, N.; Junkers, T. Kinetic Control of Aggregation Shape in Micellar Self-Assembly. *Angew. Chem.* **2019**, *131*, 13937−13940.
(52) Lerouge, S.; Berret, J. Shear-Induced Transitions and Instabilities in Surfactant Wormlike Micelles. **2009**, arXiv:0910.1854v1, pp 1−71.
(53) Bueno, R. A.; Crowley, C. M.; Hudson, S. Heterogeneous crystallization of Fenofibrate onto pharmaceutical excipients. *Cryst. Growth Des.* **2018**, *18*, 2151−2164.
(54) Buanz, A.; Gurung, M.; Gaisford, S. Crystallisation in printed droplets: understanding crystallisation of D-mannitol polymorphs. *CrystEngComm* **2019**, *21*, 2212−2219.
(55) Roelands, C. P. M.; ter Horst, J. H.; Kramer, H. J. M.; Jansens, P. J. The unexpected formation of the stable beta phase of L-glutamic acid during pH-shift precipitation. *J. Cryst. Growth* **2005**, *275*, e1389−e1395.
(56) Yu, L. Nucleation of one polymorph by another. *J. Am. Chem. Soc.* **2003**, *125*, 6380−6381.
(57) Burger, A.; Henck, J.-O.; Hetz, S.; Rollinger, J. M.; Weissnicht, A. A.; Stöttner, H. Energy/Temperature diagram and compression behaviour of the polymorphs of D-mannitol. *J. Pharm. Sci.* **2000**, *89*, 457−468.
(58) Kacker, R.; Dhingra, S.; Irimia, D.; Ghatkesar, M. K.; Stankiewicz, A.; Kramer, H. J. M.; Eral, H. B. Multiparameter Investigation of Laser-Induced Nucleation of Supersaturated Aqueous KCl Solutions. *Cryst. Growth Des.* **2018**, *18*, 312−317.
(59) Coppola, L.; Gianferri, R.; Nicotera, I.; Oliviero, C.; Ranieri, G. Structural changes in CTAB/H2O mixtures using a rheological approach. *Phys. Chem. Chem. Phys.* **2004**, *6*, 2364−2372.
(60) Du, W.; Cruz-Cabeza, A. J.; Woutersen, S.; Davey, R. J.; Yin, Q. Can the study of self-assembly in solution lead to a good model for the nucleation pathway? the case of tolfenamic acid. *Chem. Sci.* **2015**, *6*, 3515−3524.
(61) Cruz-Cabeza, A. J.; Bernstein, J. Conformational polymorphism. *Chem. Rev.* **2014**, *114*, 2170−2191.
(62) Thompson, H. P. G.; Day, G. M. Which conformations make stable crystal structures? Mapping crystalline molecular geometries to the conformational energy landscape. *Chem. Sci.* **2014**, *5*, 3173−3182.
(63) Khan, H.; Seddon, J. M.; Law, R. V.; Brooks, N. J.; Robles, E.; Cabral, J. T.; Ces, O. Effect of glycerol with sodium chloride on the krafft point of sodium dodecyl sulfate using surface tension. *J. Colloid Interface Sci.* **2019**, *538*, 75−82.
(64) Su, W.; Zhang, Y.; Liu, J.; Ma, M.; Guo, P.; Liu, X.; Wang, H.; Li, C. Molecular dynamic simulation of D-mannitol polymorphs in solid state and in solution relating with spontaneous nucleation. *J. Pharm. Sci.* **2020**, *109*, 1537−1546.

https://doi.org/10.1021/acs.cgd.1c00243
Cryst. Growth Des. 2021, 21, 3928−3935